Direct Calculation of Double Counting Rate for Neutron Multiplicity Methods

Wilfried Monange *

Grégory Caplin †

Olivier Jacquet ‡

August 5, 2020

1 Introduction

Neutron density in nuclear system is subject to fluctuations that arise from nuclear random process. For sub-critical systems with large number of neutrons these fluctuations are usually small enough so that the well known Boltzmann equation is valid and the system is correctly described by mean quantities. This is no more true with a law neutron density that implies predominantly neutron fluctuations over average values obliging the use of other techniques to correctly describe the neutron population. Among them, the Neutron Multiplicity Counting (NMC) methods [1, 2] focus on correlated time neutrons (i.e. neutrons belonging to the same fission chain) detections for sub-critical system using mean single count rate (i.e. mean count rate of detection), double count rate (i.e. mean count rate of time correlated pairs of detections), triple count rate (i.e. mean count rate of time correlated triples of detections), etc. In this way NMC is based on higher-order moment of the counting distribution.

Usually NMC values obtained by simulation are calculated with algorithms very similar to those used with real detectors and therefore only make use of detection times. Depending on the simulation tools, the calculation of these values is performed directly inside the simulation code or outside *via* output files (List-mode like) and post-processing programs. This approach is referred here to as the *analog method*. As this method require exact simulation of the transport of neutrons, i.e. analog calculation, classical Monte Carlo techniques for variance reduction (Russian roulette, splitting etc.), which only preserve first order moment (mean quantities), cannot be used.

As a consequence and although dating back to the early nuclear era, the use and study of NMC techniques has been for many years limited by the performance of computers that struggled to simulate the entire neutron population of an experiment. Thanks to modern computers a number of barriers have been raised and these techniques are now regularly used for the reactivity assessment of low power ADS reactors, non-destructive assay of special nuclear material, sub-critical benchmarks [3, 4, 5, 13], etc.

However, NMC simulations can still be very CPU time consuming under certain circumstances such as configurations with huge calculation time for neutron transport or when NMC values with large time scale are required. Some methods have been developped to solve this problem such as variance reduction techniques [6] or sensitivities estimation throw eigen values calculations [7]. This paper proposes another ap-

*Institut of Radioprotection and Nuclear Safety
†ORANO at IRSN when the work was prepared
‡Subcontractor

proach based on the use of analog simulation tools taking advantage of an additional information provided by the code : the fission chain identifier (or history identifier) to which a detection belongs. This information makes it possible to identify the correlated detections, i.e. resulting from the same fission chain. This approach will be referred to the *direct method*. The word "direct" refers to the direct identification of correlated detections. This paper focuses on the calculation of the single counting rate, the double counting rate and the so called Feynman-Y curve [8, 9].

The first part recalls the *analog method* methodology, then the theory of the direct method is described and is applied to a real experiment in the last part.

2 Analog method

The calculation of NMC values has been extensively described in the literature [10, 11]. This section recall the basis using the Hage-Cifarelli formalism [12] in order to keep consisteing with the *direct method* formalism in the next section. During an NMC simulation, neutron detections are time-tagged and stored into a file creating the so called *signal* (which therefore contains a set of detection times). In a second step, the post processing divid this *signal* into equal samples of width τ. For each of them the number of events are counted and binned into a histogram called the Feynman histogram. This histogram therefore represents the occurrence probabilities of various multiplets (i.e., 1 detection, 2 detections, etc.) occurring within a specified samples width τ. Several methods exist to split the signal, Figure 2.1 shows the construction of the Feynman histogram with consecutive samples.

From these the c_k values representing the number of times k detections are found in samples are deduced. This can be repeated for multiple samples widths resulting in multiple Feynman histograms. The NMC values are finally calculated with the following formulas:

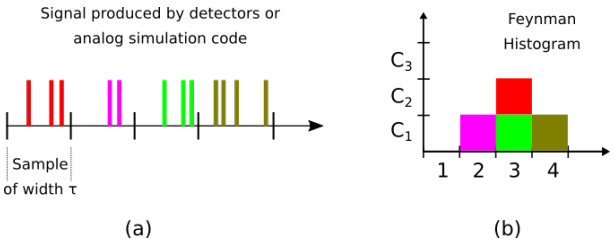

Figure 2.1: The post-processing divid a signal into samples (a) and construct the feynman histogram (b).

$$m_1(\tau) = \frac{\sum_k k\, c_k(\tau)}{\sum_k c_k(\tau)}$$

$$m_2(\tau) = \frac{1}{2}\frac{\sum_k k(k-1) c_k(\tau)}{\sum_k c_k(\tau)}$$

$$Y_1(\tau) = \frac{m_1(\tau)}{\tau}$$

$$Y_2(\tau) = \frac{1}{\tau}\left(m_2(\tau) - \frac{1}{2}m_1(\tau)^2\right)$$

$$Y(\tau) = 2 \times \frac{Y_2(\tau)}{Y_1(\tau)}$$

Where Y_1 and Y_2 stand for the single and double counting rates for samples of width τ, m_1 and m_2 being the first two reduced factorial moments as expressed in the Hage-Cifarelli formalism. Y is the Feynman-Y value also equal to the ratio of the variance to the mean in the number of neutron detections in samples of width τ minus unity : $Y(\tau) = \frac{Var(C_k(\tau))}{Mean(C_k(\tau))} - 1$.

Since $Y_1(\tau)$ is simply the count rate, his value should remain constant regardless the samples width value (as long as it is sufficiently large to avoid statistical effect) and equal to a named value R_1.

Changing τ allows to adjust the amount of detections coming from the same fission chains (i.e. correlated detections) taken into account. If τ tends towards zero the probability of having correlated detections also tends towards zero as well as $Y_2(\tau)$ and

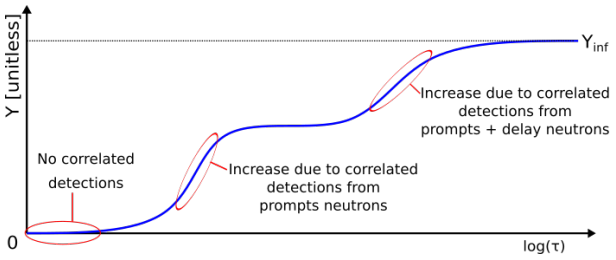

Figure 2.2: Feynman-Y curve as a function of the samples width (τ).

$Y(\tau)$. If τ increases, more and more correlated detections are taken into account leading to an increase of $Y_2(\tau)$ and $Y(\tau)$. At first only correlated detections from prompt neutrons are taken into account, then from all neutrons (prompt + delayed). This is shown by the presence of two plateaus on the Feynman curve. Further increase of τ do not add more correlated detection and both $Y_2(\tau)$ and $Y(\tau)$ tend to their asymptotic values respectively named R_2 and Y_∞.

In order to reduce uncertainties the number of samples used must be large (often several thousand). If one want to cover delayed neutron, large samples are required (at least 100 seconds) and the simulated signal can required unacceptable CPU time or experiment duration. As a consequence, R_2 and Y_∞ are in practice estimated throw formulas depending on $Y_2(\tau)$ and $Y(\tau)$, making these values dependent of both the samples width (i.e. $R_2(\tau)$ and $Y_\infty(\tau)$) and the underlying theory:

$$R_2(\tau) = \frac{1}{\omega(\tau)} Y_2(\tau) \tag{2.1}$$

$$Y_\infty(\tau) = 2\,\frac{R_2(\tau)}{R_1}$$

$$\omega\left(\lambda,\tau\right) = 1 - \frac{1-e^{-\lambda\tau}}{\lambda\tau}$$

Wehre λ is the inverse of the neutron lifetime which includes slowing-down time in the detector.

Note that for the NMC values to be meaningful and usable for other measures (calculation of total multiplication for instance), the experiment must be in a steady state, i.e. the power remains constant over time.

3 Direct method

Let S be the mean rate of source events (i.e. the mean number of histories per time unit) and p_N the probability for an history to create N detections. Both values comes from simulation results. In particular, the association of each detection with the fission chain identifier makes it possible to calculate the p_N quantity. That being said, for a stationary process the mean rate of detections from histories creating N detections is $S \cdot p_N \cdot C_N^1$ where C denotes the binomial coefficient. Summing over all possible numbers of detections gives the single rate of detections:

$$\mathring{Y}_1 = S \sum_{N=1}^{\infty} p_N \cdot C_N^1 \tag{3.1}$$

In this formula as well as for the following, the circle denotes values calculated using the *direct method*. One may note that $\mathring{Y}_1$ does not depend on any samples width values and thus it is equal to its asymptotic value $\mathring{R}_1$. To be consistent with formulas presented in section 2 the expected number of detections per samples $\mathring{m}_1$ is defined as $\mathring{Y}_1\,\tau$.

The same approach is then applied for the double counting rate. Considering the mean rate of correlated pairs triggered by the *ith* detection of histories creating N detections is $S \cdot p_N \cdot C_{N-i}^1$, the mean double counting rate created by histories having N detections is equal to:

$$S \cdot p_N \sum_{i=1}^{N-1} C_{N-i}^1 = S \cdot p_N \cdot C_N^2$$

Taking into account all histories with any number of detections gives the asymptotic mean double counting rate $\mathring{R}_2$:

$$\mathring{R}_2 = S \sum_{N=2}^{\infty} p_N \cdot C_N^2 \tag{3.2}$$

Contrary to the *analog method*, the *direct method* gives directly access to the asymptotic double counting rate without the need of intermediate formulas.

As a consequence, $\mathring{R}_2$ do not depends of neither τ or an underlying theory but only on the number of simulated histories.

We are now interested in the calculation of the non-asymptotic value of $\mathring{R}_2$, i.e. $\mathring{Y}_2(\tau)$. Let's consider a first detection in the time range $[t_1, t_1 + dt_1]$ and a second one inside $[t_2, t_2 + dt_2]$ with $t_1 < t_2$, the average number of correlated pairs of detections Q_r between two correlated detections distant of $t_2 - t_1$ is:

$$Q_r(t_2 - t_1)\, dt_1 \cdot dt_2 = \mathring{R}_2 \cdot pdf(t_2 - t_1)\, dt_1 \cdot dt_2$$

With *pdf* the probability density function of the time intervals between any pair of detections of an history i.e. the auto-correlation function. Once again the fission chain identifier provided by the simulation code allows the direct calculation of the PDF. The average counts in the time ranges $[t_1, t_1 + dt_1]$ and $[t_2, t_2 + dt_2]$ that are uncorrelated pairs of detections is equal to the product of the average detection rate:

$$Q_a(t_2 - t_1)\, dt_1 \cdot dt_2 = \mathring{R}_1{}^2\, dt_1 \cdot dt_2$$

Summing Q_r and Q_a gives the well-known Rossi-Alpha distribution Q:

$$\begin{aligned} Q(t_2 - t_1) dt_1 \cdot dt_2 &= (Q_a(t_2 - t_1) + Q_r(t_2 - t_1))\, dt_1 \cdot dt_2 \\ &= \left(\mathring{R}_1{}^2 + \mathring{R}_2 \cdot pdf(t_2 - t_1)\right) dt_1 \cdot dt_2 \end{aligned}$$

Where the subscript a and r refer to the words "accidental" and "real" as often used with the Rossi-Alpha method [1]. With Q_a and Q_r defined, one can now calculate $\mathring{m}_{2a}$ and $\mathring{m}_{2r}$ which respectively correspond to the expected number of uncorrelated or correlated pairs of detection in samples of width τ. This is achieved by summing for each detection occurring at $t_1 \leqslant \tau$ the second detections occurring at $t_2 \leqslant \tau$:

$$\begin{aligned} \mathring{m}_{2r}(\tau) &= \int_0^\tau dt_1 \cdot \int_{t_1}^\tau Q_r(t_2 - t_1) \cdot dt_2 \\ &= \mathring{R}_2 \int_0^\tau cdf(t) \cdot dt \end{aligned} \tag{3.3}$$

$$\begin{aligned} \mathring{m}_{2a}(\tau) &= \int_0^\tau dt_1 \cdot \int_{t_1}^\tau Q_a(t_2 - t_1) \cdot dt_2 \\ &= \frac{1}{2} \mathring{R}_1{}^2\, \tau^2 \end{aligned}$$

With *cdf* the cumulative density function of the time intervals between any pair of detections of an history. Combination of the previous equations gives the final expression of the doubles counting rate as calculated with the *direct method* :

$$\begin{aligned} \mathring{Y}_2(\tau) &= \frac{\mathring{m}_{2r}(\tau)}{\tau} \\ &= \frac{\mathring{R}_2}{\tau} \int_0^\tau dt \cdot cdf(t) \end{aligned} \tag{3.4}$$

Note that the definition of the Feynman-Y values as two times the ratio between the double and simple counting rate remains valid so that no specific derivation is required:

$$\mathring{Y} = 2\, \frac{\mathring{R}_2}{\mathring{R}_1}$$

$$\mathring{Y}_\infty(\tau) = 2\, \frac{Y_2(\tau)}{Y_1} \tag{3.5}$$

Back to Eq. 3.3, $\int_0^\tau cdf(t) \cdot dt$ behaves asymptotically like τ since $cdf(\tau)$ approaches unity. Let us now define a function $w(\tau)$ that approaches unity as τ tends towards infinity, and $m_2(\tau)$ the number of pairs of detections in a gate of width τ. As m_2 contains both correlated and uncorrelated pairs of detections, $m_{2r}(\tau)$, can also be written as the following :

$$\begin{aligned} m_{2r}(\tau) &= m_2(\tau) - m_{2a}(\tau) \\ &= m_2(\tau) - \frac{1}{2} m_1{}^2 \end{aligned}$$

It is now possible to express the asymptotic doubles counting rate $\mathring{R}_2(\tau)$ as a function of $w(\tau)$. The deduced equation is similar to the one obtained in Equation 2.1.

$$\mathring{R}_2(\tau) = \frac{\mathring{Y}_2(\tau)}{w(\tau)} = \frac{m_2(\tau) - \frac{1}{2} m_1^2}{\tau \cdot w(\tau)}$$

The above reasoning does not differentiate between sources. For instance, if histories are created by both spontaneous fissions and $(\alpha - n)$ reactions, S combines these two types of sources. However, for practical reasons it is sometimes interesting to differentiate sources in simulations: one may perform a set of simulations with only spontaneous fission sources and another set of simulations with only $(\alpha - n)$ sources in order to later adjust the proportion of one source type to the other. Since each of these sources creates histories which are independent from each other, Equations 3.1, 3.4 and 3.2 can be easily rewritten with source differentiation by considering that the total contribution is the sum of each individual contribution:

$$\mathring{R}_1 = \mathring{Y}_1 = \sum_i^I \left[S_i \sum_{N=1}^{\infty} p_{i,N} \cdot C_N^1 \right]$$

$$\mathring{R}_2 = \sum_i^I \left[S_i \sum_{N=2}^{\infty} p_{i,N} \cdot C_N^2 \right]$$

$$\mathring{Y}_2(\tau) = \frac{\mathring{R}_{2,i}}{\tau} \int_0^{\tau} dt \cdot cdf_i(t)$$

With the subscript i denoting the contribution of the source of type i among I sources. $\mathring{Y}(\tau)$ is still calculated through two times the ratio of $\mathring{Y}_2$ and $\mathring{Y}_1$ and no specific derivation is required.

4 Results and discussion

4.1 Case study

The case study is the Sub-critical Copper-Reflected α-phase Plutonium (SCRαP) integral benchmark experiment designed and measured by the Los Alamos National Laboratory at the National Criticality Experiments Research Center (NCERC). The experiment is detailed in [13] and presented in Figures 4.1 and 4.2. It consists in a weapon-grade plutonium sphere nested in various thicknesses of copper spherical shells and/or polyethylene spherical shells. Neutrons basically arise from spontaneous fissions and

Figure 4.1: SCRαP configuration n°15 during assembly.

$(\alpha - n)$ reactions. The correlated neutron measurement were performed using a detector system made of He^3 tubes inside high density polyethylene. Among the 16 different measured configurations, this paper will focus on configuration number 15 which has the highest k_{eff} value. It consists of the plutonium sphere surrounded by a first layer of polyethylene surrounded by 7 layers of copper. Choosing the configuration with the highest reactivity will make easier to distinguish the neutrons delayed part of $Y_2(\tau)$ and $Y(\tau)$. The calculated k_{eff} of this configuration with the Monte Carlo code MORET [14] developed at IRSN is about 0.944 (σ = 100 pcm).

4.2 General procedure for the calculation of NMC values

The general procedure used in this paper for the calculation of NMC values with the *analog method* is as follow:

Step 1: A simulation is performed considering both types of neutron sources (spontaneous fissions and $(\alpha - n)$ reactions) and imposing that all histories start (i.e. the instant of the source event) at t = 0 second. The number of source events to be simulated must be sufficient for the duration of the desired signal. For each neutron detec-

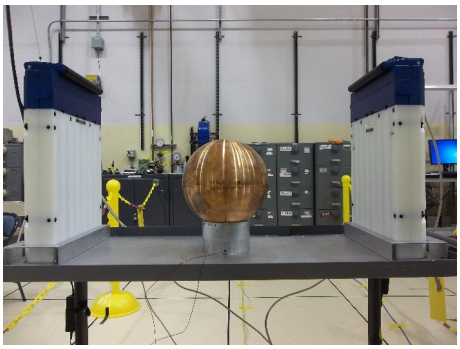

Figure 4.2: Experimental set up. The nuclear system is surrounded by the NOMAD detectors.

tion in the two NOMAD detectors, the following information is recorded:

- the type of source from which the neutron originated,
- the detection time,
- the history identifier.

The calculation has been performed using the version 6 of MORET - based on MORET 5 [14] - which allows the analog simulation of neutrons and the record of simulation information into list-mode like files.

Step 2: From the output file is extracted for each type of source a number of histories corresponding to the desired signal duration and the intensity of each source.

Step 3: The beginning of each histories (and therefore the corresponding detection times) are modified by sampling from a uniform random law over the choosen signal duration interval. Some histories may start close enough to the end of the signal so that their detection times can appear beyond the chosen signal duration. To solve this, the modulo function of parameter the signal duration is applied on each detection time to confine the detection times to the desired time interval.

Step 4: All detection times are merged to form the final signal.

Step 5: Other post-processing can be applied to simulate experimental instrumentation behavior such as the detectors dead-time or the detectors time resolution. For this present work no experimental instrumentation effect is taken into account since the *direct method* cannot handle them for the time beeing and this step is skipped.

Step 6: NMC values are calculated using post processing programs as for a signal originating from real detectors.

There is several benefits to this approach for the *analog method*. First, the simulation of the transport of one history is an independent process from the transport of other histories. Therefore, this approach does not necessarily require a parallelized computation code and it is sufficient to run several instances of the computation code, taking care to modify the seed of the random generator. Secondly, it is possible to adjust the parameters used in post-processing (sources intensities, sources types, signal duration) to build a new signal without having to recalculate the transport part whose calculation time is much longer than that of the post-processing part. Another interesting point is the possibility to change the seed used to sample the beginning time of the histories (step 3). One can then create multiple signals that all contain the same knowledge (i.e. fission chains, detections, etc.) but distributed differently (although the uniform random law is still used). This allows the study of statistical properties (expected mean and standard deviation) of observable calculated from these signals.

Regarding the *direct method* the post processing program only needs the result of the first step for the calculation of the two required terms p_N and $pdf(t)$. Since each recorded detection has been associated to its corresponding history identifier the calculation of p_N is straightforward. The calculation of $pdf(t)$, must be done taking into account all the combination of detections originating from a history as illustrated in Figure 4.3. It is important that the binning used to calculate $pdf(t)$ is fine and cover a large time range in

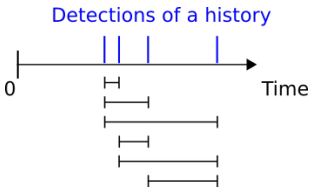

Figure 4.3: All the combination of detections originating from a history must be taken into account for the calculation of $cdf(\tau)$.

order to include both prompt and delayed neutrons. In the following comparison the binning is composed of 1000 values logarithmicaly distributed between $1 \cdot 10^{-9}$ and $1 \cdot 10^{4}$ seconds.

As seen from Equation 3.5, $Y_1(\tau)$, $Y_2(\tau)$ and $Y(\tau)$ are link to each other, moreover as no discrepancy is expected for the single counting rate, this paper focus only on the comparisons between $Y(\tau)$ and $\mathring{Y}(\tau)$.

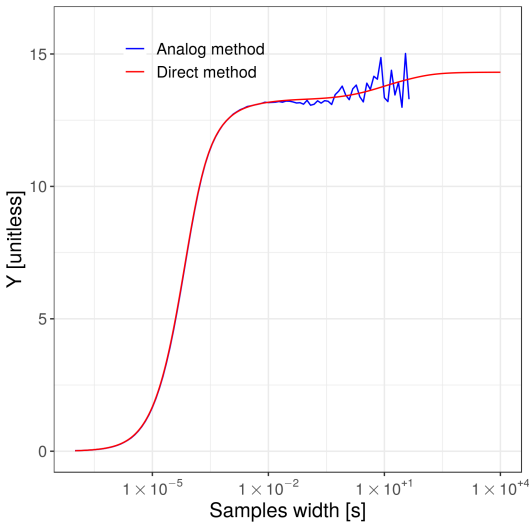

Figure 4.4: Comparison of $Y(\tau)$ and $\mathring{Y}(\tau)$ for samples widths between $1 \cdot 10^{-7}$ and $1 \cdot 10^{4}$ seconds.

4.3 Mean values comparison

According to the SCRαP benchmark report [13] neutrons arise from approximately 128500 spontaneous fissions per second and 4200 $(\alpha - n)$ reactions per second. The duration of the simulated signal is about 5500 seconds which approximately represents $7 \cdot 10^{8}$ spontaneous fissions and $2.3 \cdot 10^{7}(\alpha - n)$ reactions. A first comparison is presented in Figure 4.4 for samples widths from $1 \cdot 10^{-7}$ to $1 \cdot 10^{4}$ seconds between the *direct method* (i.e. $\mathring{Y}(\tau)$) in red and the *analog method* (i.e. $Y(\tau)$) in blue. For samples width smaller than $1 \cdot 10^{-2}$ seconds both methods are in good agreement. Above this samples width the *analog method* starts to exhibit large fluctuations (due to an insufficient number of samples used to calculate the NMC values) that makes the comparison infeasible. Futures analyses focus on samples widths greater than $1 \cdot 10^{-2}$ seconds.

A possible way to make the comparison feasible for larger samples widths is to lengthen the simulated signal duration by performing additional simulations. This methodology is in practice inaccessible for desktop computers due to the high CPU time consuming (we are speaking of orders of magnitude longer simulation duration). Another approach is to create a number of independent signals by changing the seed as explained before. The results of this method is presented in Figure 4.5 for a set of 100 independent generated signals looking at the mean (blue curve) and the standard deviation (curve named (a)) of $Y(\tau)$ values. From this figure it can be inferred that the averaged *analog* $Y(\tau)$ values are consistent with the *direct method* up to samples width of 10 seconds. This figure also shows a very good agreement between the standard deviation based on Reference [10] (curve named (b)) and based on the set of generated signals (curve named (a)). Once again lets recall that all these signals contains the same "amount of knowledge" (i.e. sames histories, detections, etc.).

To go further in the comparison, one may generate additional simulated signals. As presented in Figure 4.6, the use of 1000 generated signals (green curve) do not show any significant improvement compare to the use of 100 generated signals.

Although the previous figures tend to show consistency between the two methods, the delayed neutron part of the Feynman curve could not be compared. To access this portion another approach must be used. By reducing the intensity of the neutron

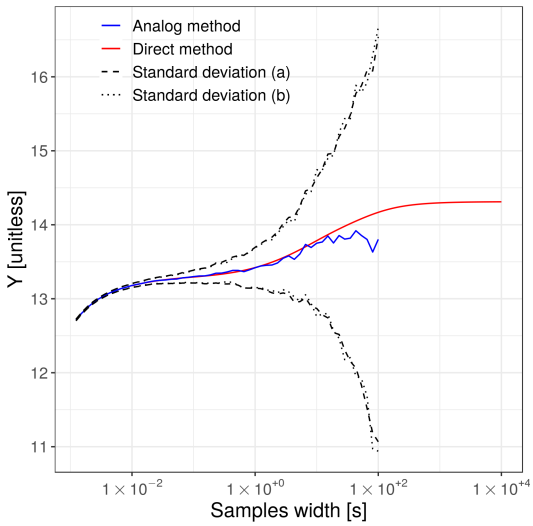

Figure 4.5: Comparison over 100 generated signals of $\mathring{Y}(\tau)$ and averaged $Y(\tau)$ values. A comprison between two methods for standard deviation estimation is also presented.

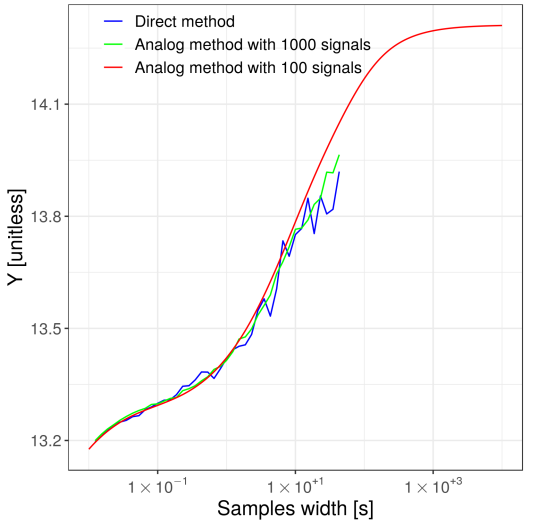

Figure 4.6: Comparison of $\mathring{Y}(\tau)$ and averaged $Y(\tau)$ values over 100 generated signals.

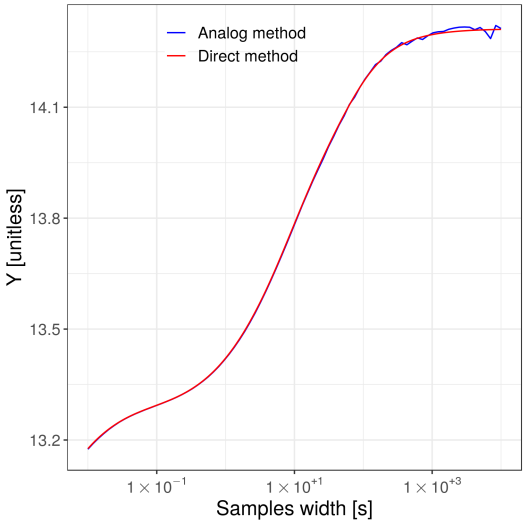

Figure 4.7: Comparison of $Y(\tau)$ and $\mathring{Y}(\tau)$ based on an extended signal.

sources it is possible to artificially lengthen the signal duration for the same number of simulated histories. It should be noted that this method does not require additional simulation (neutron transport), as the signal broadening is performed with post-processing functions. In this way, a new set of 100 signals have been generated with a duration equal to $5.5 \cdot 10^6$ seconds (about 64 days) corresponding to a source composed of 128.5 SF per second and about 4.2 $(\alpha - n)$ reactions per second. Results presented in Figure 4.7 for samples widths from $1 \cdot 10^{-2}$ to $1 \cdot 10^4$ seconds between the direct method (red curve) and the averaged $Y(\tau)$ values (blue curve) show a good agreement over all the inspected ranges.

4.4 Variance comparison

For the time being, exact formula of the variance of $\mathring{Y}(\tau)$ has not been yet established and estimation of this value is relying on multiple sets of histories. Figure 4.8 shows the variance as a function of the sets size expressed as the proportion of histories used to calculate Y from the previous plots (4.4 to 4.6). The samples width is equal to $1\,s$ and each variance value

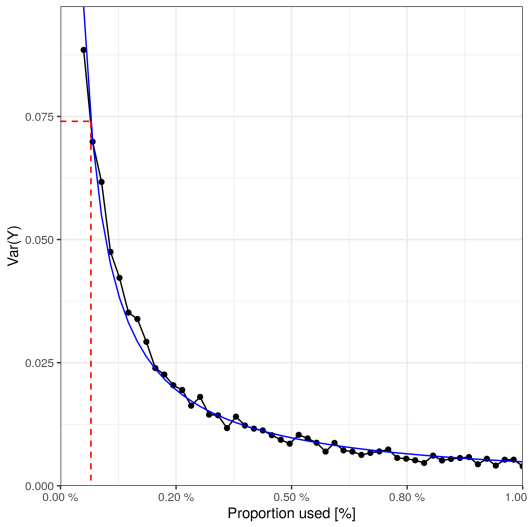

Figure 4.8: Variance of $\mathring{Y}(\tau)$ as a function of the proportion of histories used.

is calculated with 50 sets of histories. The blue line is a fit demonstrating that the variance varies as the inverse of the number of simulated histories. This is in contrast with the *analog method* whose the variance varies with the inverse of the number of samples. This figure also includes the uncertainty of $Y(\tau = 1\,s)$ from Figure 4.5 as a red dashed line (with nominal sources intensities and with all the available histories).

Taking into account that the variance of $Y(\tau = 1\,s)$ for the SCRαP experiment (Figure 4.5) is about 0.8, this figure shows that the direct method has about the same variance as the analog method using about 0.1% of the total simulated histories. It has to be noted that this gain depends on many parameters which are not presented here due to the lack of theoretical formula of the direct method's variance. Nevertheless it is obvious that this gain increase with the intensity of the signal since the fission chains tends to overlap more and more.

5 Conclusion and future work

Traditionally, NMC values are calculated using similar tools to exploit the detections obtained by the experiment's detectors or by simulation. However, in some cases this approach can be very CPU intensive. The *direct method* uses additional information provided by the simulations to significantly reduce uncertainties and thus simulation times. However, as the present situation stands, this method cannot completely replace the traditional method. The main identified limitations are the following:

- requirement of sub-critical system in a steady state (i.e. constant power with time);
- detector dead time not take into account;
- higher order of counting rates (triple, etc.) are not yet derive.

Concerning the last point, it should be noted that these values are often difficult to obtain by simulation due to the need of a high detection efficiency to keep the variance reasonable. Therefore the development of the calculation of this value with the *direct method* could be very advantageous for applications that use these types of measures.

References

[1] N. Ensslin, W. Harker, M. Krick, D. Langner, M. Pickvell: Application guide to neutron multiplicity counting, Los-Alamos manual, LA-13422-M (1998)

[2] A.A. Robba, E.J. Dowdy and H.F. Atwater, "Neutron Multiplication Measurements Using Moments of the Neutron Counting Distribution", Nuclear Instruments and Methods 215 (1983) 473-479

[3] J. Arthur, et. al. "Validating the performance of correlated fission multiplicity implementation in radiation transport codes with subcritictal neutron multiplication benchmark experiments", Annals of Nuclear Energy 120 (2018) 348-366

[4] Richard, B., Hutchinson, J., 2016. Tungsten-reflected plutonium-metal-sphere subcritical measurements. In: International Handbook of Evaluated Criticality Safety Benchmark Experiments, NEA/NSC/DOC/(95)03/I, FUND-NCERC-PU-HE3-MULT-002.

[5] Richard, B., et al., 2016. Nickel-reflected plutonium-metal-sphere subcritical measurements. In: International Handbook of Evaluated Criticality Safety Benchmark Experiments, NEA/NSC/DOC/(95)03/I, FUND-NCERC-PU-HE3-MULT-001.

[6] M. Szieberth, J.L. Kloosterman, "New Methods for the Monte Carlo Simulation of Neutron Noise Experiments in ADS".

[7] J. Hutchinson, T. Cutler, "Use of Criticality Eigenvalue Simulations for Subcritical Benchmark Evaluations".

[8] R. P. Feynman, et. al., "Dispersion of the Neutron Emission in U-235 Fission", J. Nuclear Energy, 1956, Vol. 3, pp. 64 to 69. Pergamon Press Ltd., London

[9] S. Croft et al., « Feynman variance-to-mean in the context of passive neutron coincidence counting », Nuclear Instruments and Methods In Physics Research Section A: Accelerators, Spectrometers, Detectors and Associated Equipment, Volume 686, 11 September 2012, Pages 136-144.

[10] R. Uhrig, "Random Noise Techniques in Nuclear Reactor Systems", John Wiley & Sons Inc, 1970

[11] J. Hutchinson, et. al., "Subcritical Multiplication experiments & Simulations: Overview and Recent Advances," ANS Advances in Nonproliferation Technology and Policy Conference, Santa Fe NM, September 2016.

[12] D.Cifarelli, W. Hage, "Models for a Three-Parameter Analysis of Neutron Signal Correlation Measurements for Fissile Material Assay," Nuc. Instr. Meth. A251, 550-563, 1986.

[13] J. Hutchinson, et. al., "Subcritical Copper-Reflected a-phase Plutonium (SCRaP) Measurements and Simulations" In: International Conference on Mathematics and Computational Methods Applied to Nuclear Science and Engineering, LA-UR-17-20621.

[14] B. Cochet, et. al. "Capabilities overview of the MORET 5 Monte Carlo code", Joint International Conference on Supercomputing in Nuclear Applications and Monte Carlo 2013 (SNA + MC 2013), La Cité des Sciences et de l'Industrie, Paris, France, October 27-31, 2013.

[15] Smith-Nelson, et. al. "Uncertainties of the Yn Parameters of the Hage-Cifarelli Formalism", Los Alamos Report LA-UR-15-21365, 2015.